Science of Sintering, **50** (2018) 421-432

doi: https://doi.org/10.2298/SOS1804421M

UDK 551.25; 669.14

Effect of the Degree of Plastic Deformation on the Thermal Electromotive Force of Cu-X5crni1810 Steel Thermocouple

Ivan Milićević[1], Milica Spasojević[2*)], Radomir Slavković[1], Miroslav Spasojević[3], Aleksa Maričić[3]

[1]University of Kragujevac, Faculty of Technical Sciences, Svetog Save 65, Čačak, Serbia
[2]University of Belgrade, Faculty of Chemistry, Studentski trg 12-16, Belgrade, Serbia
[3]University of Kragujevac, Joint Laboratory for Advanced Materials of SASA, Section for Amorphous Systems, Faculty of Technical Sciences, Svetog Save 65, Čačak, Serbia

Abstract:

The thermal electromotive force (TEMF) and the thermal electromotive force coefficient (TEMFC) of the thermocouple consisting of a copper wire and an (X5CrNi1810) steel wire plastically deformed under tension or bending conditions were found to increase with increasing degree of plastic deformation. The increase in the degree of deformation disturbs the microstructure of steel due to increases in the density of chaotically distributed dislocations and internal microstress, resulting in a decrease in the electron density of states near the Fermi level. Through the effect of thermal energy, annealing at elevated temperatures up to 300 ^{o}C leads to microstructural ordering along with simultaneous increases in the free electron density of states, TEMF and TEMFC. Based on the temporal change of the TEMF, the kinetics of microstructural ordering was determined. During the initial time interval, the process is a kinetically controlled first-order reaction. In the second time interval, the process is controlled by the diffusion of reactant species.

Keywords: *Thermal electromotive force; Relative strain; Electron density of states; Activation energy; Steel.*

1. Introduction

When subjected to mechanical stress, metals undergo deformation simultaneously with a change in their microstructure. The degree of short-range order decreases, while the density of chaotically distributed dislocations and internal microstress increase [1-3]. Some atoms make a transition to higher energy levels that exhibit a larger equilibrium distance between adjacent atoms and a smaller overlap of their valence orbitals, thus causing a decrease in the free electron density of states near the Fermi level [4-5]. The deformation-induced changes in the electron density of states produce changes in both the TEMF and the TEMFC of the deformed metal – another metal thermocouple [6-9].

At room temperature, the metastable state of most deformed metals as well as of steel does not transform into a stable state at an appreciable rate since thermal energy is not large enough to overcome the activation energy for microstructural ordering [10-27]. At higher temperatures, thermal energy reaches the value of the activation energy. This leads to microstructural ordering, causing an increase in the free electron density of states and changes

*) Corresponding author: smilica84@gmail.com

in the TEMF and the TEMFC [27-31]. As temperature increases, structural relaxation occurs in metals and alloys at temperatures lower than crystallization temperatures. This results in short-range ordering, which causes changes in physical and chemical properties as well as in the TEMF [16-27]. When temperature is above the crystallization temperature, nanocrystals first appear in the amorphous matrix. These nanocrystals grow into larger crystals during crystallization. The appearance and growth of crystals induce microstructural changes that affect the mechanical, magnetic and chemical properties as well as the TEMF of the material [16-27]. H. Chiriac *et al* [32-34] observed a correlation between the TEMF and the evolution of the crystallization process from an amorphous state over a nanocrystalline to a crystalline state of $Fe_{90}Cu_1Nb_3Si_{13.5}B_9$, $Fe_{90}Hf_7B_3$, $Fe_{90}Zr_7B_3$ and $Fe_{77.5}Si_{7.5}B_{15}$ alloys. They showed that the TEMF value increased from the amorphous to the crystalline state and that the maximum value for $Fe_{90}Cu_1Nb_3Si_{13.5}B_9$ was higher than the maximum values obtained for $Fe_{90}Hf_7B_3$ and $Fe_{90}Zr_7B_3$ alloys at the final stage of crystallization. The nanocrystalline phase formation produces a sharp increase followed by a slow increase from the nanocrystalline to the crystalline state in the absolute value of the TEMF [32-34]. L. Nordheim and C. J. Gorter [35] found that the TEMF of an alloy is mainly affected by the concentration of elements in solid solutions. N. J. Luiggi *et al* [36], V. Massardier *et al* [37] and S. I. Vooijs *et al* [38] examined the precipitation process in Al alloys using the Nordheim-Gorter mathematical expression. Based on the effect of plastic deformation, annealing temperature, TEMF and electrical resistivity, S. I. Vooijs *et al* [38] monitored the precipitation kinetics in an Al-AA3104 alloy and a Mg- and Cu-rich alloy 3104. They found that Al_2CuMg precipitates form at low annealing temperatures, irrespective of the extent of pre-deformation. During annealing at temperatures from 350 °C and higher, Mn-containing dispersoids are precipitated.

The objective of this study was to assess the effect of relative strain and heating temperature on the TEMF and the TEMFC, and use this effect to establish the kinetics of microstructural ordering in deformed steel wires. Another aim was to examine the possibility of determining the degree of recovery using the temperature dependence of the TEMF, and evaluating the degree of deformation of annealed steel wires, in view of the fact that deformation after annealing cannot be determined due to specific shapes and positions.

2. Materials and Experimental Procedures

In this investigation, *X5CrNi1810* steel wire specimens having a length l_0 = 400 *mm* and a diameter ∅2.8 *mm* were tested. Some of the specimens were subjected to plastic strain under a tensile load of 2000 to 3600 *N* (accuracy: ±10 *N*). Thereafter, the length of the tensioned wire *l* was measured, and the absolute strain of the wire was calculated, $\Delta l = l - l_0$, accuracy: $\pm 10^{-2}$ *mm*. Then, the relative strain ε of each specimen was determined using the expression $\varepsilon = \frac{\Delta l}{l}$. The other specimens were plastically deformed by bending the wire around a 10 *mm*-diameter cylinder.

The deformed steel specimens and the copper wire (400 *mm* in length and 3 *mm* in diameter) were joined by a mechanical method (pressing) to form thermocouples.

The compensation method in the temperature range of 0 to 300°C was used to measure TEMFs. During the measurement, a voltmeter with an internal impedance of 10^{10} Ω and a sensitivity of 10^{-5} V, and a microammeter of 0.5 μA sensitivity were used. One end of the thermocouple was immersed in a mixture of water and ice at 0 °C, and the other was placed in a furnace at a temperature of $t \pm 1$ ° C.

The temperature supplied by the furnace was controlled by a copper-constantan thermocouple located in the vicinity of the other end of the steel-copper thermocouple. The furnace was filled with argon to avoid the oxidation of the thermocouple.

3. Results and Discussion

The temperature dependence of the thermal electromotive force (TEMF) of thermocouples consisting of copper and steel wire specimens subjected to multiple levels of tensile strain is presented in Fig. 1.

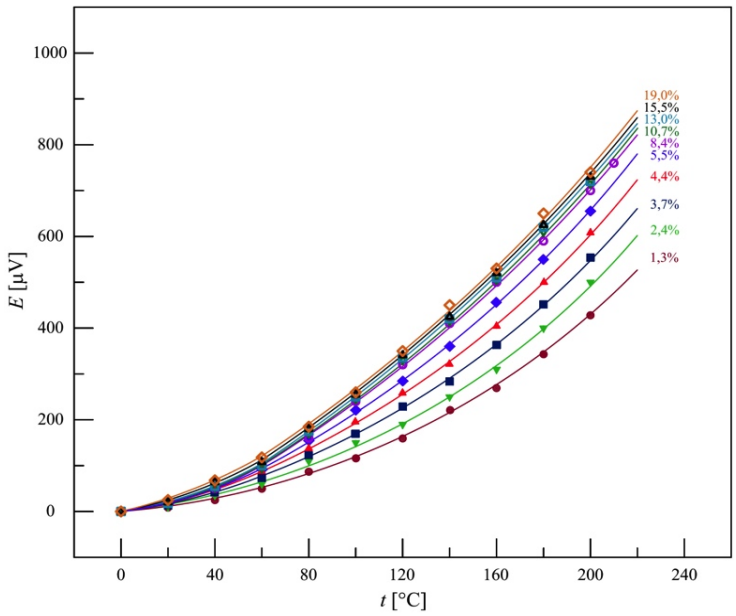

Fig. 1. Thermal electromotive force, E, of thermocouples consisting of copper and steel wire specimens subjected to multiple levels of tensile strain as a function of temperature, t, and relative strain, ε : ● - 1.3%, ▼ - 2.4%, ■ - 3.7%, ▲ - 4.4%, ◆ - 5.5%, ○ - 8.4%, ▽ - 10.7%, □ - 13.0%, △ - 15.5%, ◇ - 19.0%.
Heating rate: 20 °C min^{-1}.

As shown in the Fig., the TEMF of all specimens increases with increasing temperature. The increase is greater than linear, and the deviation is more pronounced in samples subjected to a higher strain level. The annealing process can result in the formation of a new phase as well as in the precipitation of impurities and intermetallic compounds at crystal grain boundaries. Consequently, there is a change in the chemical composition of the grain and, hence, in the TEMF. However, transmission electron micrographs of deformed samples of steel before and after annealing showed neither new phase formation nor notable precipitation. This indicated that the change in the TEMF is a plausible consequence of short-range ordering rather than phase or precipitate formation. This is the result of structural rearrangement in the material during annealing, with specimens undergoing microstructural ordering as the density of chaotically distributed dislocations and the internal microstress decrease, resulting in a better overlap of 3d and 4s orbitals, which increases the electron density of states in the conduction band near the Fermi level.

The effect of annealing temperature on the TEMF of the copper – deformed steel wire thermocouple is presented in Fig. 2, resulting in a shape similar to the curves presented in Fig. 1.

The diagrams in Fig. 1. show the thermal electromotive force coefficient (TEMFC) as a function of annealing temperature and deformation degree. The TEMFC increases with increasing temperature since thermal energy enhances the short-range ordering of the structure and, hence, the generation of electrons near the Fermi level.

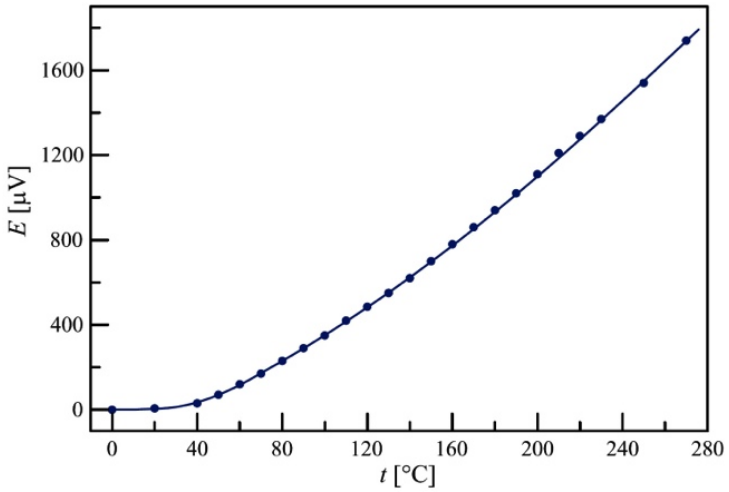

Fig. 2. Thermal electromotive force, E, of the copper - deformed loop-shaped steel wire thermocouple as a function of temperature, t.

The TEMFC also increases with increasing degree of deformation of the steel wire. At higher levels of relative strain, the density of defects is increased and, accordingly, the rate of their annihilation and the rate of generation of free electrons at elevated temperatures are higher. Increasing the density of free electrons, n_1, at the Fermi level in the steel wire causes an increase in both the TEMF and the TEMFC, in accordance with the equations:

$$E = \frac{k}{2e}\left(\frac{n_1}{n_2} - \frac{n_2}{n_1}\right)(T_2 - T_1) = \alpha \cdot \Delta T \quad (1)$$

$$\alpha = \frac{k}{2e}\left(\frac{n_1}{n_2} - \frac{n_2}{n_1}\right) \quad (2)$$

where: E (V) – thermal electromotive force (TEMF); α (V K^{-1}) – thermal electromotive force coefficient (TEMFC); k = 1.3806505·10^{-23} J K^{-1} – Boltzmann's constant; e = 1.60217653·10^{-19} C – elementary charge; n_1(cm^{-3}) – density of states of free electrons in the steel wire; n_2(cm^{-3}) – density of states of free electrons in the copper wire; T_1(K) – temperature of the hot junction of the thermocouple; T_1 = 273 K – temperature of the cold junction of the thermocouple.

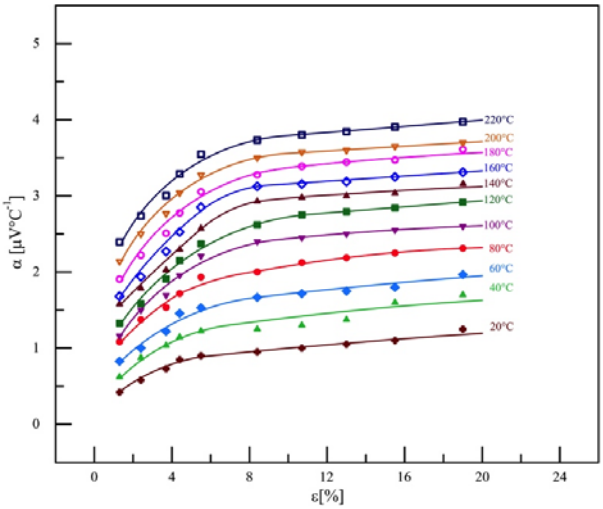

Fig. 3. TEMFC, α, as a function of temperature, t, and relative strain, ε, of steel wire specimens plastically deformed by tension: ✚ - 20°C, ▲ - 40°C, ◆ - 60°C, ● - 80°C, ▼ - 100°C, ■ - 120°C, △ - 140°C, ◇ - 160°C, ○ - 180°C, ▽ - 200°C, □ - 220°C.

The diagrams in Fig. 1. were used to determine the values of the TEMFC, α, for different temperatures and different relative strains of the steel wire plastically deformed by tension. Results are presented in Fig. 3.

Fig. 4. presents the temperature, *t,* dependence of the TEMFC, α, for a steel wire specimen plastically deformed by tension up to a relative strain of ε = 19 %, and for a steel wire specimen plastically deformed by bending around a cylinder with a diameter of d = 10 mm.

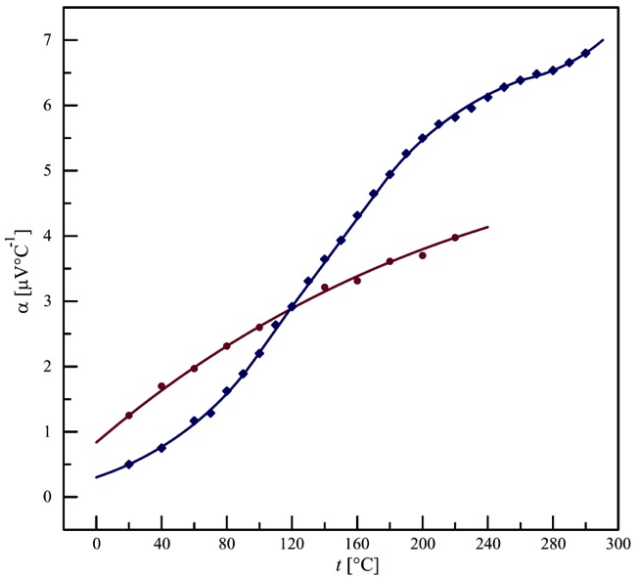

Fig. 4. TEMFC, α, as a function of annealing temperature, t, ● - steel wire specimen undergoing plastic deformation by tension up to a relative strain of ε = 19 %,◆ - steel wire specimen undergoing plastic deformation by bending around a cylinder with a diameter of d = 10 mm.

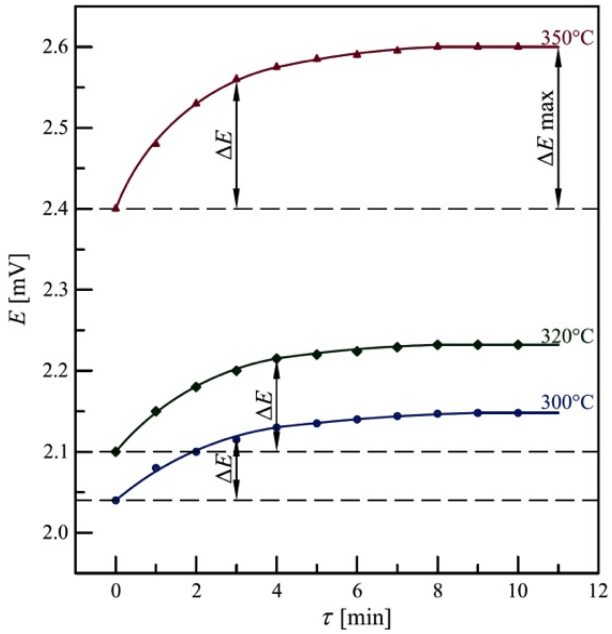

Fig. 5. TEMF, E, of the steel wire deformed by bending around a cylinder with a diameter of d = 10 mm, as a function of annealing time, τ, at temperatures: ● - 300 °C, ◆ - 320 °C, ▲ - 350 °C.

The diagrams in Fig. 4. show that, at lower temperatures, the TEMFC of the thermocouple employing a tensioned steel wire is higher than that of the thermocouple containing a bent steel wire, whereas the reverse is true at higher temperatures. This suggests that the activation energy of short-range structural ordering is lower in the tensioned wire than in the bent wire.

The recovery kinetics of the deformed steel wire was observed by measuring changes in the TEMF over time at defined temperatures. Fig. 5 presents the results of measurement at temperatures t_1= 300 °C, t_2= 320 °C and t_3= 350 °C for the wire subjected to plastic deformation by bending around a cylinder having a diameter of d = 10 mm.

The structural ordering taking place during the annealing of the deformed steel increases the density of states of free electrons near the Fermi level, thus leading to an increase in the TEMF, as expressed by the equation:

$$E_{1,\tau} - E_{1,0} = \Delta E = \frac{k}{2e}\left[\left(\frac{n_{1,0}+\Delta n}{n_2} - \frac{n_2}{n_{1,0}+\Delta n}\right) - \left(\frac{n_{1,0}}{n_2} - \frac{n_2}{n_{1,0}}\right)\right]\left(T_2 - T_1\right) \tag{3}$$

where: $E_{1,0}$- TEMF at the temperature T_2 for the time τ = 0; $E_{1,\tau}$- TEMF at the temperature T_2 after annealing of the steel specimen for the time τ ; $n_{1,0}$- density of states of free electrons in the deformed steel at the temperature T_2 for the time τ =0; $\Delta n = n_{1,\tau} - n_{1,0}$ - increment of the density of states of free electrons at the temperature T_2 during annealing for the time τ.

Rearranging Equation (3) gives:

$$\Delta E = \frac{k}{2e}\frac{\Delta n\left(n_{1,0}^2 + n_2^2 + n_{1,0}\,\Delta n\right)}{n_{1,0}\,n_2\left(n_{1,0}+\Delta n\right)}\Delta T \tag{4}$$

Given that $n_{1,0}\,\Delta n \ll n_{1,0}^2 + n_2^2$, the value $n_{1,0}\,\Delta n$ in the numerator can be neglected. Considering this assumption, as well as the assumption that $n_{1,0} \approx n_{1,0} + \Delta n$, the following expressions are obtained:

$$\Delta E = \frac{k}{2e}\frac{n_{1,0}^2 + n_2^2}{n_{1,0}^2\,n_2}\Delta T\,\Delta n \tag{5}$$

$$\Delta n = \frac{2e\,n_{1,0}^2\,n_2}{k\,\Delta T\left(n_{1,0}^2 + n_2^2\right)}\Delta E \tag{6}$$

that is:

$$\Delta n = \mathrm{K}_1\,\Delta E \tag{7}$$

Expression (7) shows that the change in the TEMF during annealing induced by structural ordering is a linear function of the change in the density of states of free electrons at the Fermi level.

Let us assume that short-range structural ordering is a first-order reaction:

$$A \rightarrow B + p\,e \tag{8}$$

and that the electron density of states after annealing for the time τ and τ = ∞ is $\Delta n = p\,C_B$ and $\Delta n_{\max} = p\,C_0$, respectively. Using these assumptions and equations, the integral form of the kinetic expression of the rate of reaction (8) was obtained:

$$\ln \frac{\frac{\Delta n_{\max}}{p}}{\frac{\Delta n_{\max}}{p} - \frac{\Delta n}{p}} = k_1 \tau \tag{9}$$

where: C_0 – initial concentration of reactant species A; C_B – concentration of species B generated after annealing time τ, k_1 – rate constant for the first-order reaction (8).

If in Equation (9) $\Delta n_{\max}$ and Δn are replaced respectively with $K_1 \Delta E_{\max}$ and $K_1 \Delta E$ (Equation 7), the following is obtained:

$$\ln \Delta E_{\max} - \ln \left(\Delta E_{\max} - \Delta E \right) = k_1 \tau \tag{10}$$

Based on the data presented in Fig. 5, values of $\ln(\Delta E_{\max} - \Delta E)$ as a function of τ at temperatures 300 °C, 320 °C and 350 °C were obtained. These values were used in plotting the diagrams presented in Fig. 6.

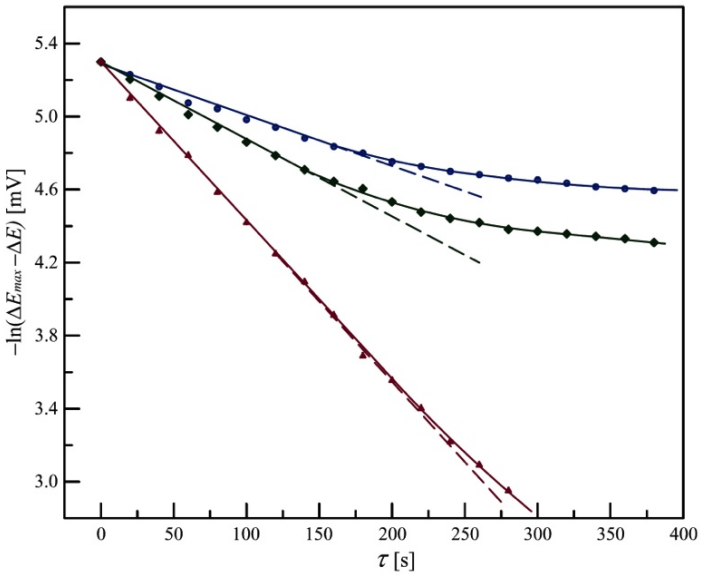

Fig. 6. Dependence of $-\ln(\Delta E_{\max} - \Delta E)$ upon time τ at temperatures: ● - 300 °C, ◆ - 320 °C, ▲ - 350 °C.

The diagrams in Fig. 6. indicate two intervals of the recovery time, with interval length depending on annealing temperature. As annealing temperature increases, the length of the first interval decreases, and that of the second one increases. In the first interval of time of 0-180 *s* at 300 °C, 0-150 *s* at 320 °C and 0-120 *s* at 350 °C, there exists a linear dependence of $ln(\Delta E_{max} - \Delta E)$ upon annealing time τ. In the second interval of time, 180-540 *s* at 300 °C, 150-480 *s* at 320 °C and 120-420 *s* at 350 °C, there is a linear dependence of ΔE upon the square root of annealing time τ (Fig. 7).

The linear dependence of $ln(\Delta E_{max} - \Delta E)$ upon annealing time indicates that, in the first interval of time, structural ordering is a kinetically controlled first-order reaction. In the second interval exhibiting a linear dependence of ΔE upon $\sqrt{\tau}$, the recovery rate of deformed steel specimens is controlled by a slow diffusion of active species. This conclusion is derived from the fact that, when diffusion becomes a slow process, Δn is a linear function of $\sqrt{\tau}$, and since $\Delta n = K_1 \Delta E$, then ΔE is also a linear function of $\sqrt{\tau}$.

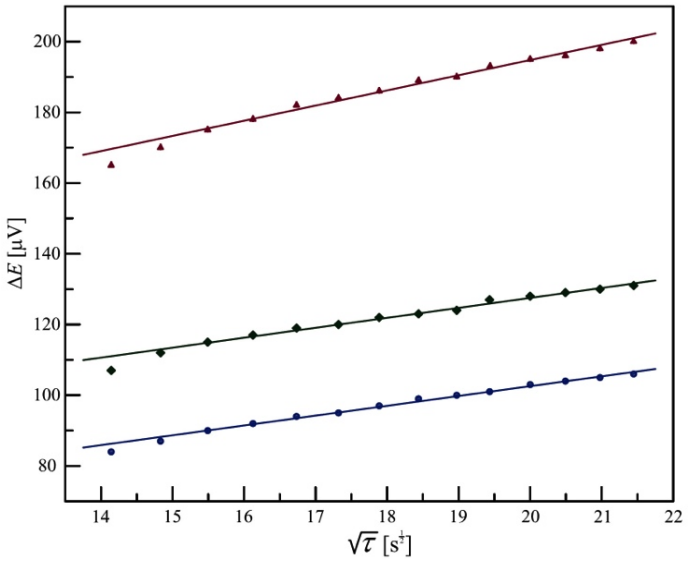

Fig. 7. Dependence of ΔE upon $\sqrt{\tau}$ at temperatures: ● - 300 °C, ◆ - 320 °C, ▲ - 350 °C.

The slopes of the lines presented in Figs. 5 and 6 give the recovery rate constants for the deformed steel wire. The rate constant of the kinetically controlled process was determined by the expression:

$$k_1 = \frac{\Delta \ln\left(\Delta E_{\max} - \Delta E\right)}{\Delta \tau} \tag{11}$$

and the rate constant of the diffusion process was determined by:

$$k_2 = \frac{\Delta E}{\Delta \sqrt{\tau}} \tag{12}$$

Based on the values obtained for k_1 and k_2, ln$k$ was plotted as a function of 1/T, and the dependence is graphically presented in Fig. 8.

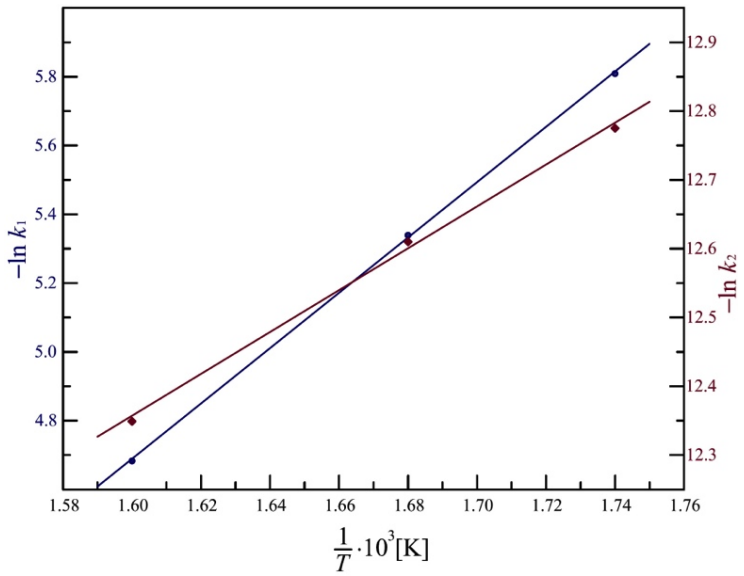

Fig. 8. Dependence of ln$k$ upon 1/T for: ● - the kinetically controlled process and ◆ - the diffusion process.

Based on the slopes of the lines given in Fig. 8, activation energies were determined for both the kinetically controlled process and the diffusion process, using the expression:

$$E_a = R\frac{\Delta(\ln k)}{\Delta\frac{1}{T}} \tag{13}$$

where: $R = 8.314$ J mol^{-1} K^{-1} – the universal gas constant
The obtained values are: activation energy of the kinetically controlled process E_{aa} = 58.7 kJ mol^{-1}; activation energy of diffusion E_{ad} = 428.7 kJ mol^{-1}.

The linear dependencies presented in Figs. 6, 7 and 8 and the values of the activation energies, E_{aa} and E_{ad}, showed that changes in the TEMF of the Cu-X5CrNi1810 steel thermocouple during the plastic deformation of steel are mainly caused by changes in short-range ordering.

4. Conclusion

The TEMF and the TEMFC of the thermocouple consisting of a copper wire and an (X5CrNi1810) steel wire plastically deformed under tension or bending conditions increase with increasing degree of plastic deformation and with rising annealing temperature. When steel is subjected to mechanical stress, the density of chaotically distributed dislocations and internal microstress increase, causing a decrease in the electron density of states at the Fermi level. Through the effect of thermal energy, short-range structural ordering takes place at elevated temperatures, accompanied by an increase in the density of states of free electrons, resulting in an increase in both the TEMF and the TEMFC. The analysis of the time dependence of the TEMF revealed that the recovery of steel is a kinetically controlled first-order reaction in the first time interval, and a diffusion-controlled reaction in the second interval of time. Activation energies were determined for both the kinetic and the diffusion process. The results presented in this paper showed that the temperature dependence of the TEMF can be successfully used to determine the degree of recovery of deformed steel wire annealed at elevated temperatures. These examples demonstrated a correlation between the temperature dependence of the TEMF and structural changes in alloys.

Acknowledgments

The authors acknowledge the financial support provided by the Ministry of Education and Science of the Republic of Serbia through Projects Ref. Nos. 172057 and TR35037.

5. References

1. Saleh AA, Pereloma EV, Gazder AA, Texture Evolution during Recrystallisation of Cold Rolled TWIP Steel, Materials Science Forum, Textures of Materials - ICOTOM 16, Vol. 702-703, December (2011) 647-650.
2. Maričić A, Spasojević M, Kalezić-Glišović A, Ribić-Zelenović L, Djukić S, Mitrović N, The stress effect on electrical resistivity sensitivity of FeBSiC amorphous ribbon, Sensors and Actuators A: Physical 174 (2012) 103-106.
3. Zeren A, Zeren M, Stress relaxation properties of prestressed steel wires, Journal of Materials Processing Technology, 141 (2003) 86-92.
4. Drobnjak Đ, Fizička metalurgija, Fizika čvrstoće i plastičnosti, Tehnološko – metalurški fakultet Univerziteta u Beogradu, Beograd, Serbia, (1990).

5. Singh J Quantum mechanics: Fundamentals and Applications to Technology, John Wiley, New York, USA, (1993).
6. Demmel P, Pazureck A, Golle R, Volk W, Hoffmann H, Characterization of the Thermoelectric Behaviour of Plastically Deformed Steels, Journal of Electronic Materials 42, 7 (2013) 2371-2375.
7. Zeren A, Effect of thermomechanical heat treatment on stress relaxation behavior of cold drawn carbon steel wires, Ph.D. Thesis, Yildiz Technical University, Istanbul, Turkey, (1993).
8. Zeren A, Kaluc E, Zeren M, Tulbentci K, Stress relaxation behaviour of thermomechanical heat treated cold drawn steel wires, Wire industry, 65, 771 (1998) 313-316.
9. Gavrilović A, Minić D, Rafailović L, Angerer P, Wosik J, Maričić A, Minić D, Phase transformations of Fe73.5Cu1Nb3Si15.5B7 amorphous alloy upon thermal treatment, Journal of Alloys and Compounds 504, 2 (2010) 462-467.
10. Jordović B, Nedeljković B, Mitrović N, Živanić J, Maričić A, Effect of Heat Treatment on Structural Changes in Metastable AlSi10Mg Alloy, Journal of Mining and Metallurgy Section B-Metallurgy, 50, 2 (2014) 133-137.
11. Minić D, Maričić A, Influence of heating on electric and magnetic properties of Fe75Ni2B13Si8C2 amorphous alloy, Materials Science and Engineering B-Advanced Functional Solid-State Materials 172, 2 (2010) 127-131.
12. Minić D, Gavrilović A, Angerer P, Minić D, Maričić A Thermal stability and crystallization of Fe89.8Ni1.5Si5.2B3C0.5 amorphous alloy, Journal of Alloys and Compounds, 482, 1-2 (2009) 502-507.
13. Minić D, Gavrilović A, Angerer P, Minić D, Maričić A, Structural transformations of Fe75Ni2Si8B13C2 amorphous alloy induced by thermal treatment, Journal of Alloys and Compounds 476, 1-2 (2009) 705-709.
14. Ristanović Z, Kalezić-Glišović A, Mitrović N, Dukić S, Kosanović D, Maričić A, The Influence of Mechanochemical Activation and Thermal Treatment on Magnetic Properties of the BaTiO3-FexOy Powder Mixture, Science of Sintering, 47, 1 (2015) 3-14.
15. Pešić O, Spasojević M, Jordović B, Spasojević P, Maričić A, Effect of Electrodeposition Current Density on the Microstructure and Magnetic Properties of Nickel-cobalt-molybdenum Alloy Powder*s*, Science of Sintering 46, 1 (2014) 117-127.
16. Spasojević M, Ribić-Zelenović L, Maričić A, Spasojević P, Structure and magnetic properties of electrodeposited Ni87.3Fe11.3W1.4 alloy, Powder Technology, 254 (2014) 439-447.
17. Spasojević M, Ćirović N, Ribić-Zelenović L, Spasojević P, Maričić A, Effect of Deposition Current Density and Annealing Temperature on the Microstructure, Hardness and Magnetic Properties of Nanostructured Nickel-Iron-Tungsten Alloys, Journal of The Electrochemical Society 161, 10 (2014) D463-D469.
18. Ribić-Zelenović L, Ćirović N, Spasojević M, Mitović N, Maričić A, Pavlović V, Microstructural properties of electrochemically prepared Ni–Fe–W powders, Materials Chemistry and Physics 135, 1 (2012) 212-219.
19. Ribić-Zelenović L, Spasojević M, Maričić A, Ristić M, The Effect of Structural Changes during Sintering on the Electric and Magnetic Traits of the Ni96.7Mo3.3 Alloy Nanostructured Powder, Science of Sintering, 41, 2 (2009) 175-184.
20. Maričić A,. Spasojević M, Ribić-Zelenović L, Mitrović N, Effect of structural changes during annealing on the electric and magnetic properties of Fe81B13Si4C2 amorphous alloy, Journal of Optoelectronics and Advanced Materials, 11, 8 (2009) 1088-1093.

21. Ribić-Zelenović L, Rafailović L, Spasojević M, Maričić A, Correlation between electron state density change and the electrical resistivity and magnetic permeability changes in the nanostructured powder of the NiMo alloy, Physica B-Condensed Matter, 403, 12 (2008) 2148-2154.
22. Ribić-Zelenović L, Rafailović L, Maričić A, Spasojević M, Correlation between electron state density change and the electrical resistivity and magnetic permeability changes in the nanostructured powder of the NiMo alloy, Journal of Optoelectronics and Advanced Materials, 9, 9 (2007) 2681-2685.
23. Soldatov AI, Soldatov AA, Kostina MA, Kozhemyak OA, Experimental Studies of Thermoelectric Characteristics of Plastically Deformed Steels ST3, 08KP and 12H18N10T, Key Engineering Materials, 685 (2016) 310-314.
24. Đorđević A R, Olćan D I, Obradović N, Paunović V, Filipović S, Pavlović V B, Electrical Properties of Magnesium Titanate Ceramics Post-Sintered by Hot Isostatic Pressing, Science of Sintering, 49, 4 (2017) 373-380.
25. Milinčić R, Spasojević M, Spasojević M, Maričić A, Ranđić S, Amorphous-Crystalline Ni-Fe Powder Mixture: Hydrogenation and Annealing Effects on Microstructure and Electrical and Magnetic Properties, Science of Sintering, 48, 3 (2016) 343-351.
26. Ćirović N, Spasojević P, Ribić-Zelenović L, Mašković P, Maričič A, Spasojević M, Synthesis, Structure and Properties of Nickel-Iron-Tungsten Alloy Electrodeposits PART II: Effect of Microstructure on Hardness, Electrical and Magnetic Properties, Science of Sintering, 48, 1 (2016) 1-16.
27. Soldatov A, Seleznev A, Fiks I, Kröning Kh, Nondestructive proximate testing of plastic deformations by differential thermal EMF measurements, Russian Journal of Nondestructive Testing, 48, 3 (2012) 184-186.
28. Soldatov AA, Control of the plastic deformation by thermo-electric method, Journal of International Scientific Publications: Materials, 5, 3 (2011) 148-155.
29. Riess I, Safadi R, Zilberstein E, Tuller HL, Differential thermal analysis of individual specimens by thermal EMF measurement, Journal of Applied Physics, 69, 3 (1991) 1205-1215.
30. Amuzu JKA, The effect of tensile stress on the thermoelectric E. M. F. in copper, gold and silver, Physica Status Solidi (a), 63, 1 (1981) K7-K10.
31. Kislyakov SA, Effect of plastic deformation and quenching on the absolute thermal emf of nickel, Soviet Physics Journal, 14, 6 (1971) 780-783.
32. Chiriac H, Inoue A, Barariu F, Nagasevschi V, Thermoelectromotive force of amorphous magnetic Fe-Cu-Nb-Si-B, Fe-Hf-B and Fe-Zr-B ribbons during the crystallization process, Mater. Sci. Eng.: A, 226-228, (1997) 650-653.
33. Barariu F, Chiriac H, Thermoelectromotive force in nanocrystalline wires, Nano Struc. Mater. 12 (1999) 650-653
34. Chiriac C, Sorohan M, Barariu F, Thermoelectromotive force of amorphous magnetic wires during crystallization, J. Phys. D: Appl. Phys. 28 (1995) 831-834.
35. Nordheim L and Gorter CJ, Bemerkungen über thermokraft und widerstand, Physica, 2, 1 (1935) 383-390.
36. Luiggi NJ, Isothermal precipitation of commercial 3003 Al alloys studied by thermoelectric power, Metall. Mater. Trans. B, 28, 1 (1997) 125-133.
37. Massardier V, Epicier T, Merle P, Proceedings of the Sixth International Conference on Aluminum Alloys: Their Physical and Mechanical Properties, edited by Sato T et al (Toyohashi: Japan Institute of light Metals), (1998) 831-836.
38. Vooijs SI, Davenport SB, Todd I, van der Zwaag S, Monitoring the precipitation reactions in a cold-rolled Al-Mn-Mg-Cu alloy using thermoelectric power and electrical resistivity measurements, Phil. Mag. A. 81 (2001) 2059-2072.

Садржај: *ТЕМС и ТКТЕМС термопара бакар-пластично деформисана (истезањем или савијањем) челична (X5CrNi1810) жица расту са порастом степена пластичне деформације и температуре загревања. Током механичког напрезања челика расте густина хаотично распоређених дислокација и унутрашња микронапрезања, што узрокује смањење густине стања електрона на Ферми нивоу. Дејством топлотне енергије на повишеним температурама уређује се структура на кратко уз повећање густине стања слободних електрона, што се одражава на повећање ТЕМС-а и ТКТЕМС-а. Анализом временске зависности ТЕМС-е установљено је да је опорављање челика у првом временском интервалу детерминисано кинетички контролисаном реакцијом првог реда, а у другом процесом дифузије. Одређене су енергије активације кинетичког и дифузионог процеса.*

Кључне речи: *термоелектромоторна сила, напрезање, густина стања електрона, енергија активације, челик.*